DIVISION S-2—SOIL CHEMISTRY

Selenate and Selenite Sorption on Iron Oxides: An Infrared and Electrophoretic Study

Chunming Su* and Donald L. Suarez

ABSTRACT

We studied selenate and selenite sorption by amorphous Fe oxide [am-Fe(OH)$_3$] and goethite (α-FeOOH) as a function of time (25 min–96 h), pH (3–12), ionic strength (0.01–1.0 *M* NaCl), and total Se concentration (0.0001–1.0 *M*). We examined sorbed selenate and selenite by in situ attenuated total reflectance Fourier transform infrared (ATR–FTIR) spectroscopy, diffuse reflectance infrared Fourier transform (DRIFT) spectroscopy, and electrophoresis to deduce sorption mechanisms. Sorption of both selenate and selenite reached equilibrium in <25 min and the sorption isotherm was not reversible. Increasing ionic strength decreased selenate sorption but did not affect selenite sorption. The presence of either selenate or selenite lowered the electrophoretic mobility (EM) and decreased the point of zero charge (PZC) of both sorbents, suggesting inner-sphere complexation for both selenate and selenite species. Both in situ ATR–FTIR and DRIFT difference spectra showed bidentate complexes of selenate with am-Fe(OH)$_3$. The structure of selenite complexes in am-Fe(OH)$_3$–solution interface was uncertain due to insensitivity of the in situ ATR–FTIR technique. The DRIFT spectra of selenite on am-Fe(OH)$_3$ showed ν_3 splitting as evidence of complexation. The DRIFT spectra of selenite on goethite showed bridging bidentate complex of selenite. We conclude that the influence of ionic strength on Se sorption cannot be used as a criterion for distinguishing outer- vs. inner-sphere complex formation.

Although Se is essential to humans and animals, it is toxic at high concentrations (NRC, 1983). Soil Se is derived from parent rocks in which Se often occurs together with sulfides in reduced forms. Weathering of parent materials causes Se oxidation and mobilization (Ihnat, 1989; McNeal and Balistrieri, 1989). Selenium deficiency has been linked to certain endemic diseases in China (Tan and Huang, 1991), whereas Se enrichment in soils and waters has been implied as a major factor resulting in severe teratogenic symptoms in wildlife at Kesterson National Wildlife Refuge in the western San Joaquin Valley, California. The source of Se to the Kesterson Wildlife Refuge is from agricultural drainage from seleniferous soils (Presser and Barnes, 1984, 1985; Letey et al., 1986). A major effort has been directed to the study of Se sorption phenomena because it plays an important role in mobility, transport, transformation, and the ultimate fate of Se in soil and aquatic systems. The interaction of the inorganic Se species, selenate and selenite with soils, individual soil components, and specimen minerals has been extensively studied and different sorption behavior found (e.g., Benjamin, 1983; Hansmann and Anderson, 1985; Balistrieri and Chao, 1987; Neal et al., 1987a,b). Selenate has been shown to behave like sulfate with minimal sorption and high mobility (Hayes et al., 1987; Goldberg and Glaubig, 1988; Neal and Sposito, 1989), while selenite behaves analogously to phosphate, with greater sorption than selenate (Neal et al., 1987a; Barrow and Whelan, 1989; Zhang and Sparks, 1990). The mechanisms of Se sorption, however, remain poorly understood.

The use of spectroscopic techniques has generated valuable yet controversial information on the structure of sorbed Se species on mineral surfaces. Harrison and Berkheiser (1982) studied the bonding mechanism of selenate with freshly precipitated hydrous ferric oxide by dispersive infrared (IR) spectroscopic analysis on air-dried samples. They concluded that selenate forms a bidentate bridging complex by replacement of protonated and unprotonated hydroxyls. The influence of air drying on the structure of surface-sorbed selenate has not been previously studied. Drying samples has been suggested as to favoring the conversion of monodentate to bidentate phosphate complexes (Goldberg and Sposito, 1985). A transition from outer-sphere to inner-sphere complex upon air drying has also been postulated for nitrate and chloride ions (Parfitt and Russell, 1977). Early evidence of the sulfate binuclear bridging inner-sphere surface complex on Fe oxides was based on infrared spectroscopy of dry materials (Parfitt and Smart, 1977).

Hayes et al. (1987) concluded, using in situ extended x-ray absorption fine structure (EXAFS) spectroscopy, that selenate forms an outer-sphere surface complex on goethite (α-FeOOH). Outer-sphere surface complexes contain at least one water molecule between the sorbate anion and the surface functional group. The low affinity of selenate for oxide surfaces has been demonstrated by the fact that selenate can be easily displaced by adding competing anions or by increasing the ionic strength with NaCl (Dzombak and Morel, 1990; Davis and Kent, 1990). Consequently, the ionic strength dependence (independence) of anion distribution at the solid–solution interface has been used as a macroscopic criterion for

C. Su, current address: ManTech Environmental Research Services Corp., R.S. Kerr Environmental Research Center, 919 Kerr Research Drive, Ada, OK 74821-1198; D.L. Suarez, USDA-ARS, U.S. Salinity Lab., 450 W. Big Springs Road, Riverside, CA 92507-4617. Received 8 Dec. 1997. *Corresponding author (su.chunming@epa.gov).

Published in Soil Sci. Soc. Am. J. 64:101–111 (2000).

Abbreviations: ATR–FTIR, attenuated total reflectance–Fourier transform infrared; DRIFT, diffuse reflectance infrared Fourier transform; EM, electrophoretic mobility; EXAFS, extended x-ray absorption fine structure; ICP-AES, inductively coupled plasma-atomic emission spectrophotometry; IR, infrared; PZC, point of zero charge.

the formation at the molecule scale of outer-sphere (inner-sphere) surface complexes (Hayes et al., 1987; Hayes and Leckie, 1987; Hayes et al., 1988). Contrary to the early findings of Hayes et al. (1987), Manceau and Charlet (1994) concluded in a recent EXAFS study that selenate forms an inner-sphere binuclear bridging surface complex on hydrous ferric oxide and goethite. Thus, the validity of using ionic strength effect to derive complexation mechanisms is questionable.

One important factor affecting ion sorption behavior is the surface charge density of sorbent particles. The surface charge characteristics of Fe oxides depend on both the surface hydroxyl density and the surface density of specifically sorbed anions. The specifically sorbed anion contributes additional negative charge to the surface, thereby displacing the point of zero charge (PZC) to lower pH values (Sposito, 1984). Microelectrophoresis is a convenient macroscopic technique for monitoring the surface charge of dispersed particles. The measurement of electrophoretic mobility (EM), which is related to the zeta potential at the shear plane and surface charge density of the sorbent particles, and the determination of PZC provide information on the nature of the surface of sorbents (Hunter, 1981).

We hypothesize that both selenate and selenite are sorbed on Fe oxides via ligand exchange and produce direct coordination to the Fe cations. In situ ATR–FTIR spectroscopy has been successfully used to study protonation of phosphate on goethite surfaces (Tejedor-Tejedor and Anderson, 1986, 1990), surface facilitated degradation of tetraphenylboron in smectite clay pastes (Hunter and Bertsch, 1994), coordination of sorbed boron on the surfaces of amorphous Al and Fe oxides and allophane (Su and Suarez, 1995), and sorption of carbonate on Al and Fe oxides (Su and Suarez, 1997a). This technique is useful to determine if the ligands are within the coordination sphere. Previous IR studies on selenate interaction with Fe oxide involved air drying of samples; however air drying may result in conversion of one surface species to another. Therefore, application of in situ ATR–FTIR spectroscopy to selenate and selenite sorption in mineral-water suspensions is preferred to examination of dry samples. Also, a comparison of IR spectra using diffuse reflectance infrared Fourier transform (DRIFT) spectroscopy is desirable for evaluating humidity effects on the structure of Se interfacial species.

The objectives of this study were to determine the bonding mechanisms of selenate and selenite with hydrous Fe oxide and goethite and to elucidate the structure of surface sorbed Se species using FTIR spectroscopy and microelectrophoresis.

MATERIALS AND METHODS

Materials

We synthesized x-ray amorphous Fe hydroxide [am-$Fe(OH)_3$] by the method of Su and Suarez (1995). Goethite was prepared by the method of Schwertmann and Cornell (1991) with an OH/Fe molar ratio of 9.0 for the parent solution using 1.0 *M* $Fe(NO_3)_3$ and 5.0 *M* KOH. The suspension of titrated $Fe(NO_3)_3$ was incubated at 70°C for 60 h and centrifuged. The goethite particles were resuspended in deionized water, the suspension pH was adjusted to 6.5 with HCl and the crystals were washed repeatedly with deionized water until the supernatant electrical conductivity was <0.003 dS m^{-1}. The solids were dried at 70°C and gently ground.

Electrophoretic Mobility

The EM was determined for minerals by microelectrophoresis using a Zeta-Meter 3.0 system (Zeta Meter, Long Island City, NY)[1]. Suspensions containing 0.2 g L^{-1} solid in 0.01 *M* NaCl with or without analytical grade Na_2SeO_4 or Na_2SeO_3 (Sigma Chemical, St. Louis, MO) were acidified to pH 3.0 with HCl and equilibrated for 1 h before being titrated with 0.01 *M* NaOH (CO_2 free) to various pH values for EM determination. The EM was determined for at least 30 particles at each pH level for each mineral. The PZC was determined by direct observation or by interpolating the data to zero mobility.

Sorption Envelopes

Batch equilibrium sorption experiments were conducted at 23°C for constructing graphs of Se sorption as a function of pH (sorption envelopes). Mineral suspensions of 4.0 g L^{-1} were prepared by adding 0.10 g of solids to either 25 mL of 0.01, 0.1, and 1.0 *M* NaCl containing Na_2SeO_4 or Na_2SeO_3 at total Se concentrations of 0.1 and 1.0 m*M*. The suspension pH was adjusted with dilute HCl or NaOH. The suspensions were shaken for 24 h and centrifuged. The supernatant solutions were analyzed for pH using a combination pH electrode, then filtered through 0.1 μm Whatman filter membraness before Se determination by inductively coupled plasma-atomic emission spectrophotometry (ICP–AES).

Sorption-desorption Isotherms

Sorbents of 0.1 g were added to 25 mL of 0.01 *M* NaCl each containing 0, 1.0, 2.0, 4.0, 6.0, 8.0, and 10.0 m*M* total selenate or selenite for am-$Fe(OH)_3$ (0, 0.1, 0.2, 0.4, 0.6, 0.8, and 1.0 m*M* for goethite) and shaken for 24 h. The suspension pH was maintained at 5.0 with dilute NaOH or HCl by continuous manual adjustment. Suspensions were centrifuged and supernatant solutions filtered prior to Se analysis by ICP-AES. Selenium sorbed by the minerals was calculated as the difference between the initial and equilibrium Se concentrations.

Desorption was initiated from each sorption mineral suspension by replacing the removed aliquot with 25 mL of 0.01 *M* NaCl. The solids were resuspended by vigorous agitation and equilibrated on a reciprocating shaker for 24 h. Although pH values of the suspensions after solution replacement were found to decrease by <0.3 units, they were nevertheless adjusted to and maintained at 5.0 by NaOH addition. After equilibration the suspension was centrifuged and the filtered supernatant was analyzed for Se. This procedure was repeated three times, resulting in a total of four desorption steps for each sorption sample. The amount of desorption was corrected for the carry-over from each previous desorption.

ATR–FTIR Spectroscopy

Infrared spectra of the aqueous solutions of Na_2SeO_4 and Na_2SeO_3, and selenate, or selenite-sorbent suspensions were recorded in the 4000 to 700 cm^{-1} range with a Bio-Rad FTS-

[1] Mention of trade names is for the benefit of the reader only and does not indicate endorsement by the USDA.

7 spectrometer equipped with Balston H_2O/CO_2 stripper, a deuterated triglycine sulfate detector, and a CsI beamsplitter (Digilab, Cambridge, MA) or a Bio-Rad FTS-175C spectrometer equipped with Balston H_2O/CO_2 stripper, a deuterated triglycine sulfate detector or MCT detector and a KBr beamsplitter (Digilab, Cambridge, MA). An ATR apparatus with a horizontal reservoir as a sample holder and a ZnSe crystal rod with a 45 degree angle of incidence was used for sample analysis. The sample reservoir was made of stainless steel and had a volume of 4 mL. Single beam IR spectra were developed from 2000 co-added interferograms with a 4 cm^{-1} resolution after purging the sampling chamber with filtered air for 30 min. All final spectra were obtained by subtracting either the spectra of the supernatant or the ionic strength and pH-adjusted deionized water solutions using NaCl, HCl, and NaOH (reference) from spectra of the sorbent suspensions or Na_2SeO_4 and Na_2SeO_3 in solution (sample), respectively (Tejedor-Tejedor and Anderson, 1986). Both reference and sample spectra were ratioed against empty reservoir cell spectra. A unity subtraction factor was always used. Four grams of am-$Fe(OH)_3$ (or 2.0 g of goethite) were added to 20 to 30 mL of 1.0 *M* NaCl, 0.05 *M* Na_2SeO_4 + 1.0 *M* NaCl, 0.10 *M* Na_2SeO_4 + 1.0 *M* NaCl, 0.5 *M* Na_2SeO_3 + 1.0 *M* NaCl, or 1.0 *M* Na_2SeO_3 + 1.0 *M* NaCl. All the solutions were adjusted to pH 5.0 or 8.0. The suspension pH was adjusted to 5.0 and 8.0 manually with 1.0 *M* HCl and 1.0 *M* NaOH, and readjusted to the target values (within 0.02 pH units) 30 min before centrifugation. The amount of hydroxyl release as a result of Se sorption was determined as the amount of HCl consumed during the sorption experiment to maintain the pH at 5.0 and 8.0, respectively, after correcting for the amount of HCl or NaOH consumed by the minerals in the Se-free 1.0 *M* NaCl to achieve the same pH. The suspensions were shaken for 24 h and centrifuged and 3.2 mL of the supernatant was used as a reference for ATR–FTIR examination. The am-$Fe(OH)_3$ solid was resuspended in the remaining 4 or 8 mL (10 mL for goethite) of the supernatant in the centrifuge tube and used as the sample. This procedure yields a solid concentration of 1000 or 500 g L^{-1} in the ATR reservoir for am-$Fe(OH)_3$ and 200 g L^{-1} for goethite. Preliminary experiments using concentrations of 500 to 1000 g L^{-1} showed that it was necessary to decrease goethite concentrations to avoid gel formation that is undesirable when using the ATR reservoir. The remaining solid suspensions were washed with 30 mL of deionized water four times and then air dried. A subsample of 5 mg was used for the DRIFT analysis. The amount of sorbed Se in the washed mineral samples was determined by digesting a subsample of 50 mg in 50 mL of 1.0 *M* HNO_3 at 90°C and measuring Se by ICP-AES.

DRIFT Spectroscopy

Samples subjected to ATR–FTIR study were also examined by the DRIFT spectroscopy to evaluate the effects of air drying on the structure of interfacial Se species. Infrared spectra of mineral solids were recorded with the same Bio-Rad FTS-7 FTIR or Bio-Rad FTS-175C spectrometers. The spectra were presented in terms of diffuse absorbance instead of the commonly used Kubelka-Munk or remission function. Aochi and Farmer (1992) have shown that spectral subtraction produces less noise in the difference spectra, and the qualitative changes in the spectra are much more easily observed using diffuse absorbance over Kubelka-Munk mode. Band intensities in diffuse absorbance show relative rather than absolute quantities (Nguyen et al., 1991). Water-washed minerals were air dried in the centrifuge tubes for 48 h, and a subsample of 5 mg was hand ground for 3 min and mixed with 95 mg of fine KBr. Alternatively, "wet samples" (4 mg dry weight) were

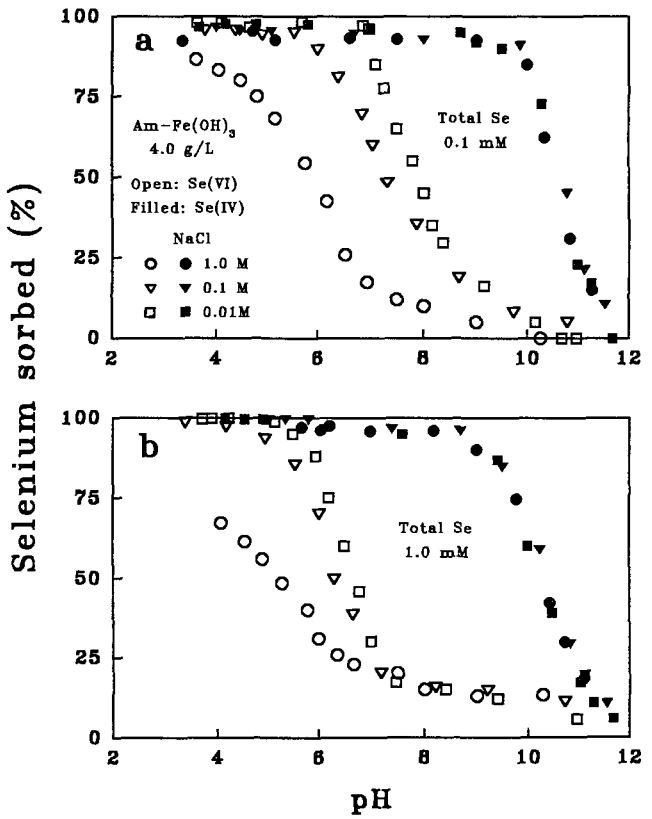

Fig. 1. Percent of the total Se added to solution that is sorbed to am-$Fe(OH)_3$ as a function of pH and ionic strength with (a) 0.1 m*M* total Se, and (b) 1.0 m*M* total Se. The solid concentration was 4.0 g L^{-1}.

removed from the centrifuge tubes and a subsample of 5 mg was mixed with 95 mg of fine KBr. Wet samples were 40% water by weight. Stainless steel cylindrical sample cups (2 by 7 mm i.d.) were filled with the KBr-diluted sample powder and the sample surface was leveled with a glass slide. DRIFT spectra were recorded from 4000 to 200 cm^{-1} at 4 cm^{-1} resolution over 500 scans after purging the sample chamber with filtered, dry air for 10 min, eliminating interference by CO_2 and water vapor (Su and Suarez, 1997b).

Other Characterization Techniques

The starting minerals and deionized water-washed minerals previously reacted with Na_2SeO_4 and Na_2SeO_3 were examined by x-ray diffraction. Deposited minerals on glass slides were scanned in 0.02° 2θ steps with a Philips model 12045 diffractometer (Philips Electronic Instruments, Mount Vernon, NY) using Cu kα radiation and a LiF crystal monochromator. Specific surface areas of sorbents were determined using a single-point BET N_2 adsorption isotherm on a Quantachrome Quantasorb Jr. surface area analyzer (Quantachrome Corp., Syosset, NY).

RESULTS AND DISCUSSION

Batch Sorption and Desorption

The sorption reaction of both selenate and selenite by am-$Fe(OH)_3$ and goethite at pH 5.0 was fast, reaching equilibrium within 25 min, the minimum time required for separation of solids and solution by centrifugation and filtration (data not shown). More selenite than sele-

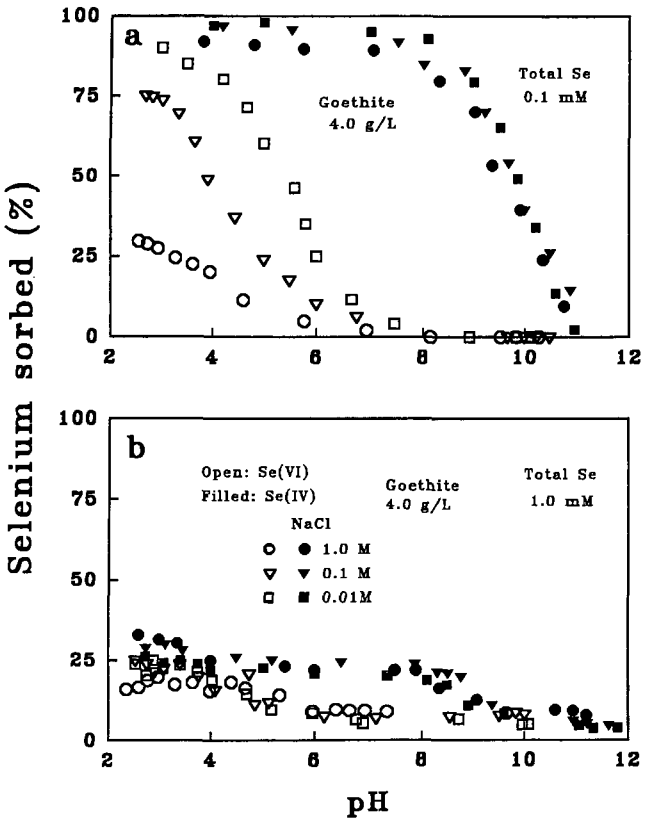

Fig. 2. Percent of the total Se added to solution that is sorbed to goethite as a function of pH and ionic strength with (a) 0.1 m*M* total Se, and (b) 1.0 m*M* total Se. The solid concentration was 4.0 g L^{-1}.

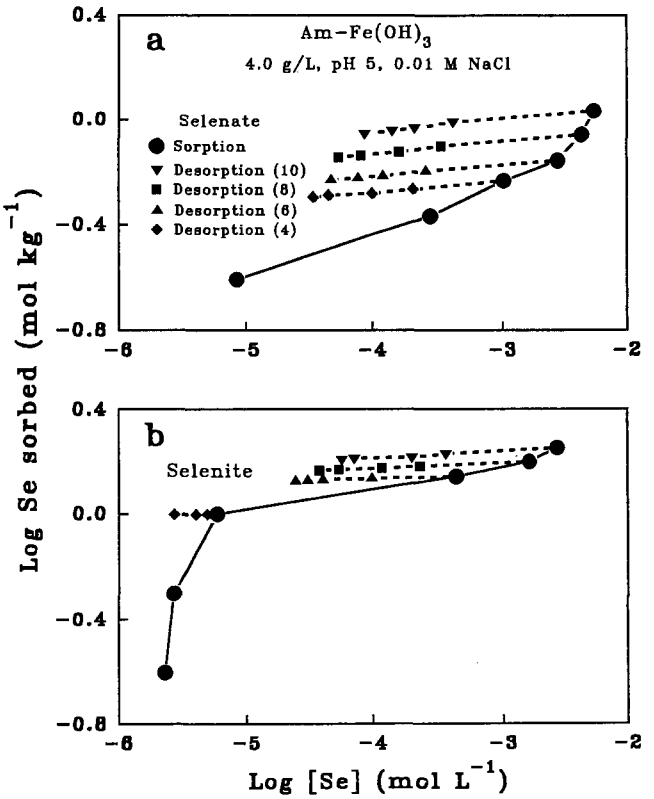

Fig. 3. Sorption–desorption isotherms for am-Fe(OH)$_3$ in 0.01 *M* NaCl at pH 5.0, showing natural logarithm of Se sorbed as a function of the logarithm of the equilibrium Se concentration: (a) selenate and (b) selenite. The solid concentration was 4.0 g L^{-1}. Desorption was performed following centrifugation of suspensions after a 24-h equilibration for sorption. Each desorption process involved a 24-h equilibration in 0.01 *M* NaCl at pH 5.0 followed by centrifugation. Numbers in parantheses represent initial selenate concentrations of 4, 6, 8, and 10 m*M*.

nate was sorbed by goethite, whereas similar amounts of selenite and selenate (>95% of total Se) were sorbed by am-Fe(OH)$_3$.

Ionic strength did not influence the sorption of selenite onto am-Fe(OH)$_3$ at a total Se concentration of 0.1 m*M* (Fig. 1a) or 1.0 m*M* (Fig. 1b). While an increase in ionic strength from 0.01 to 1.0 *M* dramatically decreased selenate sorption (Fig. 1a and 1b). In addition, an increase in the total Se concentration from 0.1 to 1.0 m*M* in am-Fe(OH)$_3$ suspensions shifted the sorption edge to the lower pH values. In the goethite suspensions at 0.1 m*M* total Se concentration, selenate and selenite sorption envelopes were well separated and a slight ionic strength effect on sorption was observed for selenate (Fig. 2a). At 1.0 m*M* total Se concentration, a two-order magnitude change in ionic strength had little effect on selenate sorption (Fig. 2b) and flat sorption envelopes were evident for both selenate and selenite. This was due to an excess of the sorbate and insufficient surface sites for sorption on goethite, as the BET N_2 surface area was 250 and 21.8 $m^2\ g^{-1}$ for am-Fe(OH)$_3$ and goethite, respectively. No negative sorption of selenate was observed even at pH > 10, in contrast to the sorption of nitrate and chloride, which show negative sorption at high pH (Wang et al., 1987; Zhang et al., 1996).

The presence or absence of an ionic strength effect on selenate sorption provides only macroscopic information on the relative affinity of selenate for Fe oxide surfaces compared to other ions, and no molecular level structural information can be deduced with confidence. In fact, an increase in ionic strength has been shown to decrease sorption of anions including phosphate (Barrow and Ellis, 1986), selenite (Barrow and Whelan, 1989a), molybdate (Goldberg et al., 1997), borate (Goldberg et al., 1993), and carbonate (Van Gee et al., 1994), all known to form inner-sphere complexes. Manceau and Charlet (1994) questioned the relevance of the ionic strength dependence (independence) of sorption isotherms as a criterion used to differentiate between outer-sphere (inner-sphere) complex formation. Although a measure of anion-bonding affinity for oxide surface, the effect of ionic strength on anion sorption on oxide surfaces provides no reliable information on bonding mechanisms at the solid–water interface. The ionic strength effect on anion sorption can be explained by the mass-action principle and activity of ions in solution without invoking detailed molecular structure of the sorbed anion species on mineral surfaces (McBride, 1997).

Selenate and selenite sorption–desorption isotherms were presented in Fig. 3 and 4. Greater amounts of selenite than selenate were sorbed by either am-Fe(OH)$_3$ or goethite. More Se was sorbed on am-Fe(OH)$_3$ than on goethite. Desorption data points deviated significantly

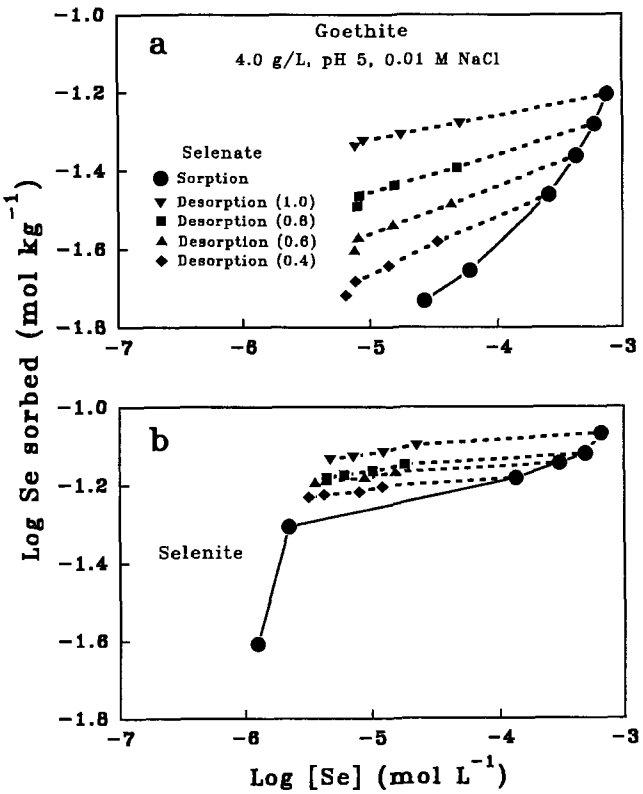

Fig. 4. Sorption–desorption isotherms for goethite in 0.01 *M* NaCl at pH 5.0: (a) selenate and (b) selenite. Experimental conditions were the same as in Fig. 3 except that the initial Se concentrations were one-tenth of those for am-Fe(OH)$_3$.

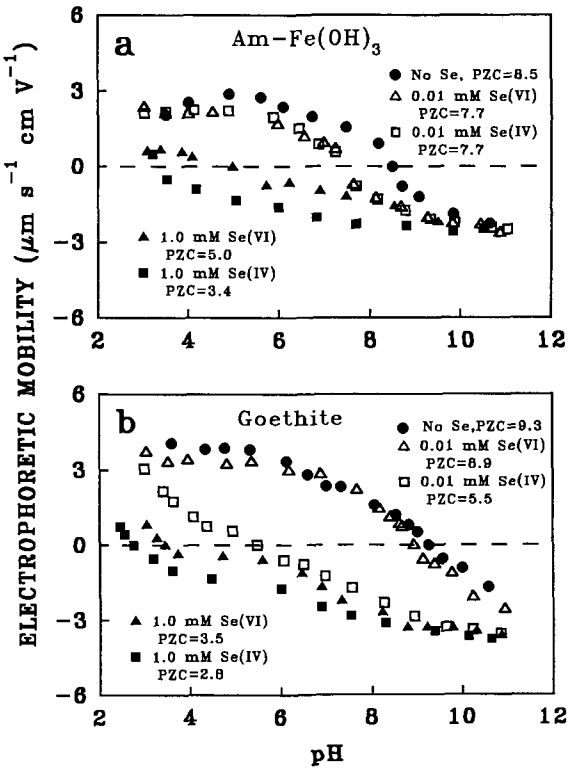

Fig. 5. Electrophoretic mobility of (a) am-Fe(OH)$_3$ and (b) goethite in 0.01 *M* NaCl with and without added Se. The suspensions were acidified to pH 3.0 with HCl and then titrated with 0.01 *M* NaOH. Initial solid concentration was 0.2 g L^{-1}.

from the corresponding sorption isotherms, indicating hysteretic desorption. This would argue against an outer-sphere complexation mechanism for selenate sorption. If such a mechanism is correct, then a greater amount of sorbed selenate should desorb.

Electrophoretic Mobility

The presence of either selenate or selenite decreased the EM and shifted the PZC of both am-Fe(OH)$_3$ and goethite to lower pH values. Depending on the surface species proposed this may imply inner-sphere complexation of both selenate and selenite with both sorbents (Fig. 5). Similar results were reported for phosphate sorbed on goethite (Tejedor-Tejedor and Anderson, 1986), for borate (Su and Suarez, 1995) and carbonate (Su and Suarez, 1997a) sorbed on Al and Fe oxides. Electrophoresis cannot distinguish between adsorption and surface precipitation nor can it identify monodentate or bidentate surface complexes. Electrophoretic mobility is, however, complementary to the spectroscopic techniques from which direct information of molecular interactions between sorbate and sorbent can be obtained.

Free Selenate and Selenite Ions in Aqueous Solution

ATR-FTIR difference spectra of 0.1 *M* Na_2SeO_4 in 1.0 *M* NaCl at pH 8.0 and of 1.0 *M* Na_2SeO_3 in 1.0 *M* NaCl at pH 5.0 and 8.0 are shown in Fig. 6. A single peak at 872 cm^{-1} was also identified for selenate at pH 5.0 (data not shown). The peak was attributed to the free SeO_4^{2-} anion because this anion is the only predominant species at pH 5.0 and 8.0. This is consistent with the ionization reaction of selenic acid, with a pKa_2 of 1.97 (Elrashidi et al., 1987) and the fact that SeO_4^{2-} does not polymerize in Na_2SeO_4 solution in the absence of other complexing agents. The vibration spectrum of the SeO_4^{2-} anion can be interpreted on the basis of a tetrahedron (four oxygen nearest neighbors), which has a T_d symmetry (Ross, 1972; Nakamoto, 1986). The band at 872 cm^{-1} was assigned to ν_3 (asymmetric stretching of Se-O bond). Ross (1972) gives the Raman spectra of free SeO_4^{2-} in solution as follows: ν_1 (symmetric stretching of Se-O) at 837 cm^{-1}, ν_2 (in-plane bending of Se-O) at 345 cm^{-1}, ν_3 (asymmetric stretching of Se-O) at 873 cm^{-1}, and ν_4 (out-of-plane bending of Se-O) at 314 cm^{-1}. Only ν_3 and ν_4 are IR active (Nakamoto, 1986) but ν_4 was not observed in the ATR study because it is beyond the IR detection range of the ZnSe crystal.

High concentrations of Na_2SeO_3 were used because concentrations below 0.1 *M* gave very weak unsatisfactory IR absorbance peaks. The solutions of Na_2SeO_3 at pH 5.0 give two absorbance bands near 850 and 825 cm^{-1}, whereas an additional band at 731 cm^{-1} was observed at pH 8.0. The four normal modes of vibrations of a pyramidal SeO_3^{2-} are both IR and Raman active (Ross, 1972; Nakamoto, 1986). Both mononuclear and binuclear species are present in concentrated Na_2SeO_3 solutions. Distribution of Se species in 1.0 *M* $NaClO_4$

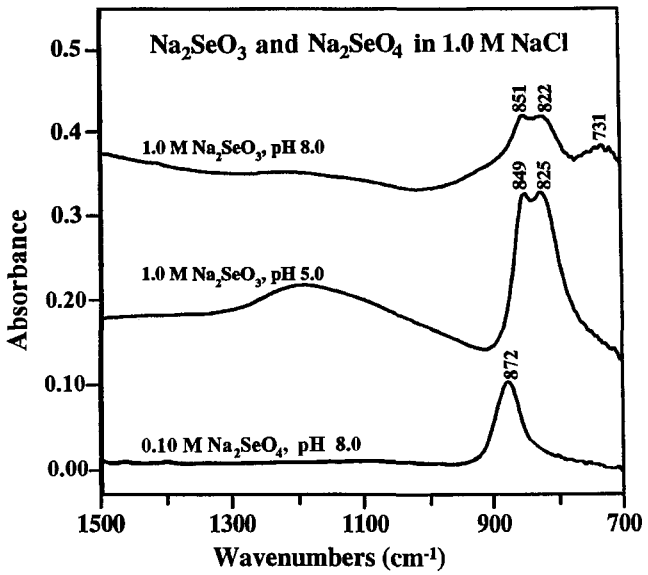

Fig. 6. The attenuated total reflectance–Fourier transform infrared (ATR–FTIR) difference spectra of selenate and selenite in aqueous solution (spectrum of 0.1 *M* Na_2SeO_4 or 1.0 *M* Na_2SeO_3 in 1.0 *M* NaCl at pH 5.0 or 8.0 − spectrum of 1.0 *M* NaCl at pH 5.0 or 8.0). The subtraction factor was unity. The spectra are offset for clarity.

with total Se at 1.0 *M* Na_2SeO_3 at pH 5.0 are 56% $HSeO_3^-$ and 44% $H_2(SeO_3)_2^{2-}$, and at pH 8.0 are 32% SeO_3^{2-}, 28% $H_2(SeO_3)_2^{3-}$, 24% $H_2(SeO_2)_2^{2-}$ and 16% $HSeO_3^-$ (Barcza and Sillen, 1971). The SeO_3^{2-} anion is dominant only at pH >10 where selenite sorption on Fe oxides started to decrease with increasing pH, resulting in insufficient amount of sorption to give satisfactory IR signals. No assignments to individual selenite species were made due to the presence of multiple selenite species in the solution.

Characterization of Interfacial Selenate

Free selenate ion belongs to the T_d point group and shows ν_3 and ν_4 fundamental IR bands. When selenate coordinates to a metal cation, the symmetry of selenate decreases, resulting in a splitting of the ν_3 band. If a monodentate complex (C_{3v} symmetry) forms, two bands appear and if a bidentate complex (C_{2v} symmetry) forms, three bands are present (Harrison and Berkheiser, 1982; Table 1). To distinguish between a bidentate chelate and a bidentate bridging complex, a comparison with known complexes can be made (Harrison and Berkheiser, 1982). Following a method of Tejedor-Tejedor and Anderson (1986, 1990), we obtained the spectra of chemical species at the solid–aqueous solution interface by subtracting the bulk solution (supernatant) IR absorption from the spectrum of the corresponding sorbent suspension. The resulting difference spectra contain IR absorption bands due to both solid bulk and interfacial species. The difference ATR–FTIR spectra of am-$Fe(OH)_3$ reacted with 0.05 and 0.1 *M* Na_2SeO_4 at pH 5.0 (Fig. 7) show two bands at 895 and 885 cm^{-1}, indicating a reduction in symmetry. Indication of mono- or bidentate complex is not definitive, but the spectra around 900 to 880 cm^{-1} can only be simulated by three peaks 890, 879, and 824 cm^{-1} from spectral deconvolution of the difference spectra (b–c) (Fig. 8). The DRIFT difference spectra of am-$Fe(OH)_3$ reacted with 0.05 and 0.1 *M* Na_2SeO_4 at pH 5.0 (Fig. 9) show clearly three bands at 916, 890, and 820 cm^{-1} attributable to a reduction in symmetry of adsorbed selenate ion. Further spectra were collected with the FTS-175C by repeating the experiment with fresh am-$Fe(OH)_3$ and 0.1 *M* Na_2SeO_4 solution. After reaction the Fe oxide suspensions were centrifuged and the wet material (40% water by weight) was mixed with KBr as before. At this time new spectra

Table 1. Infrared absorption bands of selenate and selenite in the mineral–solution interface (ATR–FTIR) and on air-dried mineral surfaces (DRIFT). According to Fowless and Stranks (1977) the distinction between monodentate and bidentate selenito complexes is that the monodentate selenito complexes show weak to medium broad bands, whereas bridging bidentate selenito complexes show medium to strong sharp absorbance bands.

Anion-complex	Symmetry	Absorption frequency, cm^{-1}				Reference
		ν_1	ν_2	ν_3	ν_4	
Free SeO_4^{2-}	T_d			872		This study
Monodentate selenate						
$[CoSeO_4(NH_3)_5]Cl$	C_{3v}	800	345	885, 845	412, 395	Ross and Thomas (1970)
Bridging bidentate selenate						
$[Co_2(SeO_4)_2OH(NH_3)_6]Cl$	C_{2v}	801		908, 872, 822		Weighardt and Eckert (1971)
Am-$Fe(OH)_3$-selenate (ATR-FTIR)				890, 879, 824		This study
Am-$Fe(OH)_3$-selenate (DRIFT)				916, 891, 824		This study
Am-$Fe(OH)_3$-selenate (DRIFT, wet)				915, 891, 824		This study
Goethite-selenate (DRIFT)				911, 885, 815		This study
Free SeO_3^{2+}	C_{3v}	807	432	737	374	Nakamoto (1986)
H_2SeO_3	C_s	831	702	430	336	Nakamoto (1986)
Monodentate selenite						
Cis-$[Co(en)_2(H_2O)HSeO_3](ClO_4)_2{\cdot}H_2O$†	C_s	830	530	770, 580	400, 350	Fowless and Stranks (1977)
Trans-$[Co(En)_2(H_2O)HSeO_3](ClO_4)_2{\cdot}H_2O$	C_s	830	520	760, 600	380, 360	Fowless and Stranks (1977)
Bridging bidentate selenite						
$[Co(en)_2SeO_3]ClO_4{\cdot}H_2O$	C_s	830	515	762, 678	405, 360	Fowless and Stranks (1977)
$[Co(tn)_2SeO_3]ClO_4{\cdot}H_2O$‡	C_s	832	520	762, 673	390, 362	Fowless and Stranks (1977)
Am-$Fe(OH)_3$-selenite (ATR-FTIR)		844		750		This study
Am-$Fe(OH)_3$-selenite (DRIFT) (pH 5)		842	594	757	478	This study
Am-$Fe(OH)_3$-selenite (DRIFT) (pH 8)		838		760, 710	472, 390	This study
Goethite-selenite (DRIFT)		886	532	778, 656	453	This study

† en = ethylenediamine
‡ tn = 1,3-propanediamine.

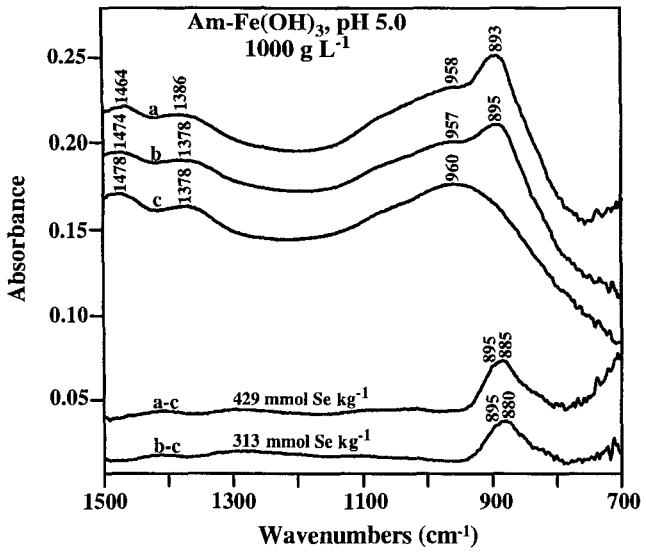

Fig. 7. The attenuated total reflectance–Fourier transform infrared (ATR–FTIR) difference spectra of am-Fe(OH)$_3$ equilibrated at pH 5.0 with (a) 0.1 *M* Na_2SeO_4 + 1.0 *M* NaCl, (b) 0.05 *M* Na_2SeO_4 + 1.0 *M* NaCl, and (c) 1.0 *M* NaCl alone. The BET N_2 surface area of am-Fe(OH)$_3$ was 250 $m^2\ g^{-1}$.The subtracted reference spectra were the supernatant solutions. The initial solid concentration was 200 g L^{-1} before centrifugation and the solid concentration in the ATR reservoir was 1000 g L^{-1}. The interfacial selenate spectra were presented as (a–c) and (b–c), respectively.

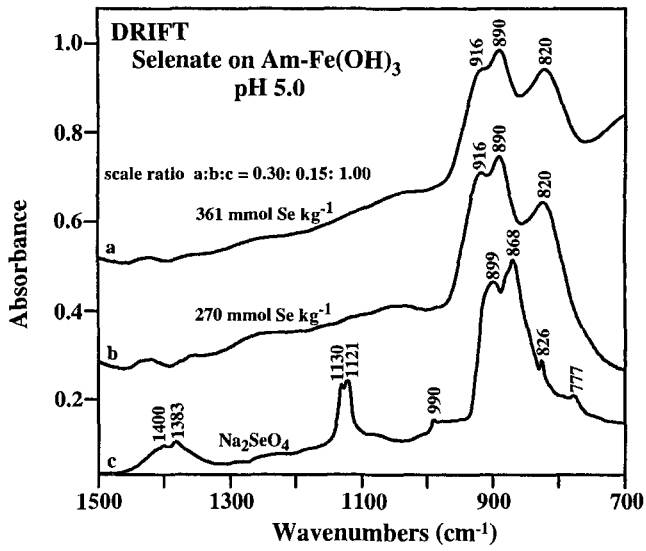

Fig. 9. Diffuse reflectance infrared Fourier transform (DRIFT) difference spectra of sorbed selenate on am-Fe(OH)$_3$ reacted at pH 5.0 with (a) 0.10 *M* Na_2SeO_4 + 1.0 *M* NaCl, and (b) 0.05 *M* Na_2SeO_4 + 1.0 *M* NaCl. The reference spectrum for (a) and (b) was the am-Fe(OH)$_3$ equilibrated with 1.0 *M* NaCl. The solid to KBr ratio was 5 to 95 mg. Regent grade Na_2SeO_4 (c) was included for comparison. The BET N_2 surface area of am-Fe(OH)$_3$ was 250 $m^2\ g^{-1}$.

were also collected for the same material only air dried (as in Fig. 9). The spectra presented in Fig. 10 also showed the presence of three peaks at 915, 891, and 823 cm^{-1} for both the wet and air-dried systems. No evidence of biselenate ($HSeO_4^-$) species was obtained for the interfacial region of am-Fe(OH)$_3$ suspension because IR bands characteristic of ($HSeO_4^-$) near 948, 870, 702, and 444 cm^{-1} (Ross, 1972, p. 225) were absent. On the contrary, the DRIFT spectra clearly show the triplet splitting of the ν_3 band when selenate sorbed onto am-Fe(OH)$_3$ at pH 5.0 (Fig. 8 and 9). This demonstrates the strong coordination of the selenate anion to the iron cation (Table 1). Pure Na_2SeO_4 shows two bands at 1400 and 1383 cm^{-1} which are probably due to CO_3^{2-} or NO_3^- impurity as pointed out by Sathianandan et al. (1964). The origin of the two bands at 1121 and 1130 cm^{-1} is unknown and was observed also by Sathianandan et al. (1964). A bidentate bridging complex is thus supported by a comparison of these bands with those

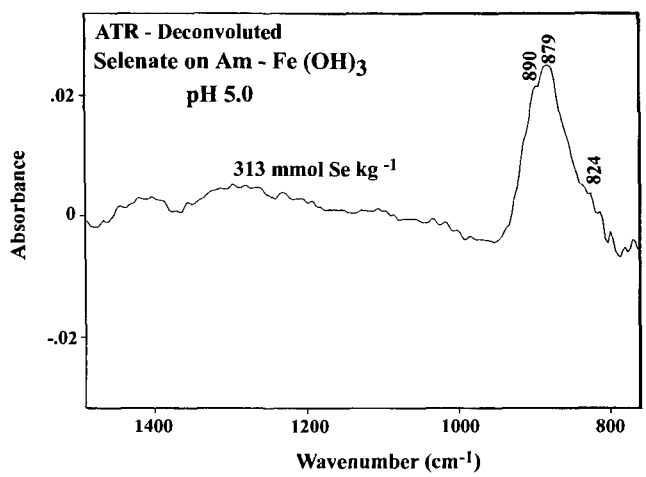

Fig. 8. Spectral deconvolution of the attenuated total reflectance–Fourier transform infrared (ATR–FTIR) difference spectra (b–c) from Fig. 7.

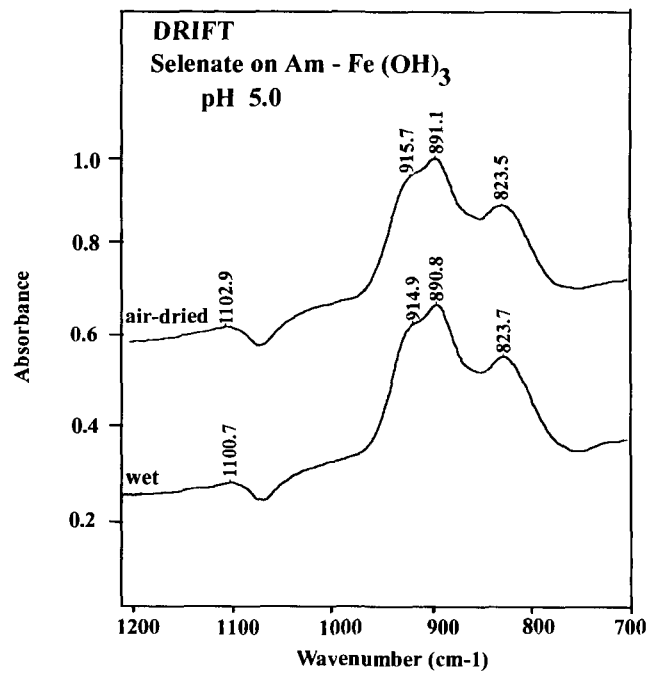

Fig. 10. Diffuse reflectance infrared Fourier transform (DRIFT) difference spectra of sorbed selenate on am-Fe(OH)$_3$ reacted at pH 5.0 with 0.01 *M* Na_2SeO_4 + 1.0 *M* NaCl. Spectra were collected for both wet (40% water by weight) and air-dried Fe oxide suspensions using a Bio-Rad FTS-175C immediately after mixing with KBr at a solid to KBr ratio of 5 to 95 mg.

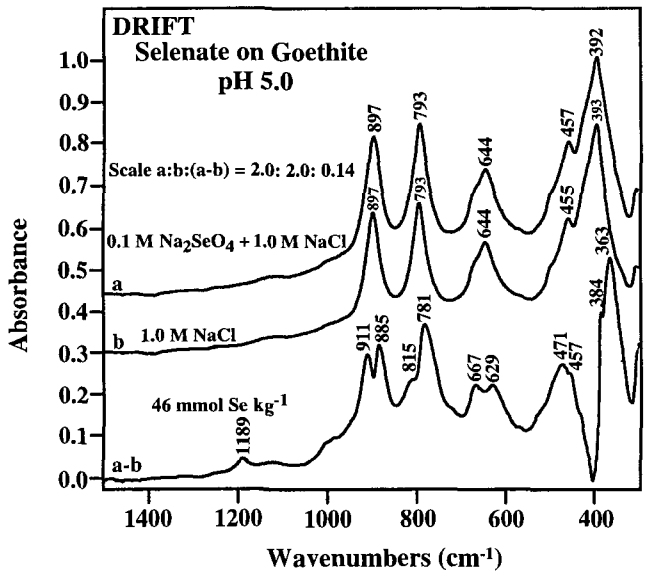

Fig. 11. Diffuse reflectance infrared Fourier transform (DRIFT) spectra of goethite reacted at pH 5.0 with (a) 0.10 *M* Na_2SeO_4 + 1.0 *M* NaCl, and (b) 1.0 *M* NaCl alone, and the difference spectrum (a–b). The solid to KBr ratio was 5 to 95 mg. The BET N_2 surface area of goethite was 21.8 $m^2\ g^{-1}$.

for the Co(III) bidentate bridging compound (Table 1). A bidentate bridging complex was also suggested by Harrison and Berkheiser (1982) for selenate sorbed on am-$Fe(OH)_3$ using air-dried samples. We note that the peak at 820 cm^{-1} is prominent in the DRIFT spectra but not in the ATR spectra. We conclude that selenate forms a bidentate bridging complex on the am-$Fe(OH)_3$ surface under dry conditions and to a lessor extent in

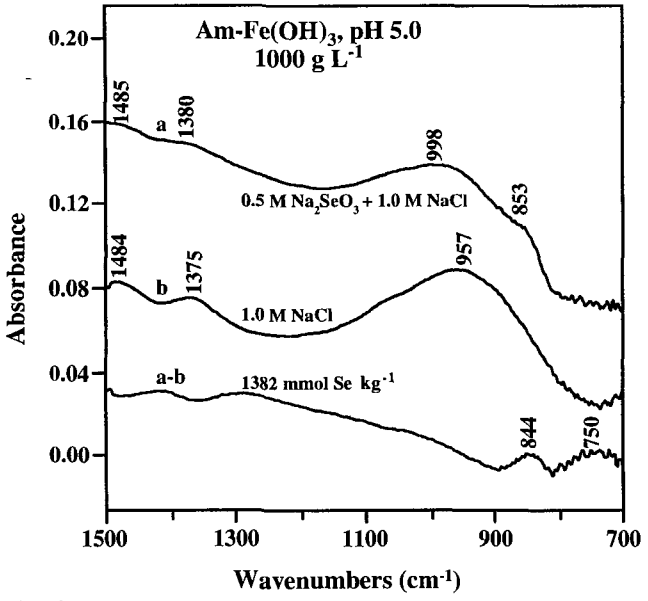

Fig. 12. Attenuated total reflectance–Fourier transform infrared (ATR–FTIR) difference spectra of am-$Fe(OH)_3$ equilibrated at pH 5.0 with (a) 0.5 *M* Na_2SeO_3 + 1.0 *M* NaCl, and (b) 1.0 *M* NaCl alone. The subtracted reference spectra were the supernatant solutions. The initial solid concentration was 200 g L^{-1} before centrifugation and the solid concentration in the ATR reservoir was 1000 g L^{-1}. The interfacial Se(IV) spectrum was presented as (a–b).

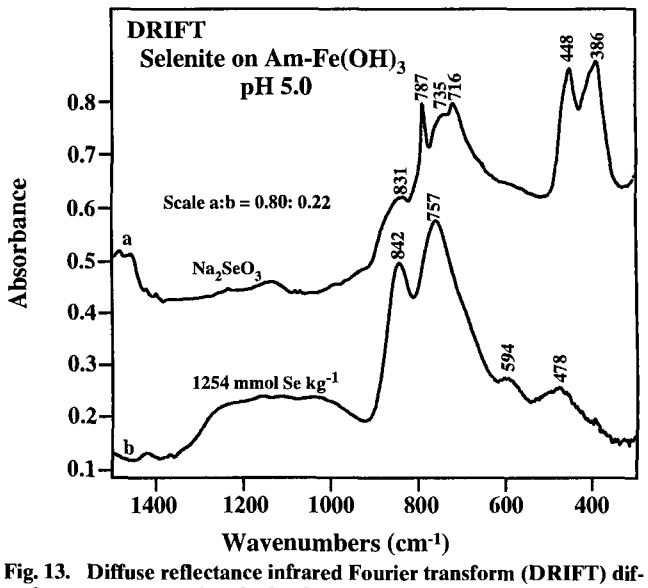

Fig. 13. Diffuse reflectance infrared Fourier transform (DRIFT) difference spectra of sorbed selenite on am-$Fe(OH)_3$ reacted with 0.05 *M* Na_2SeO_3 + 1.0 *M* NaCl at pH 5.0. The reference spectrum was the am-$Fe(OH)_3$ equilibrated with 1.0 *M* NaCl.

aqueous suspension. These spectra are consistent with a mixture of mono- and bidentate complexes.

In comparison with am-$Fe(OH)_3$, goethite was less reactive with selenate and selenite as shown by their lower amounts of sorption. This is largely due to the much smaller surface area of goethite relative to am-$Fe(OH)_3$. No detectable IR absorption bands were found for either selenate or selenite species in the interfacial region of goethite for the concentrations examined. The DRIFT spectra of goethite with and without selenate (Fig. 11) showed little difference with strong absorbance bands for the goethite lattice. The DRIFT difference spectra between selenated and nonselenated

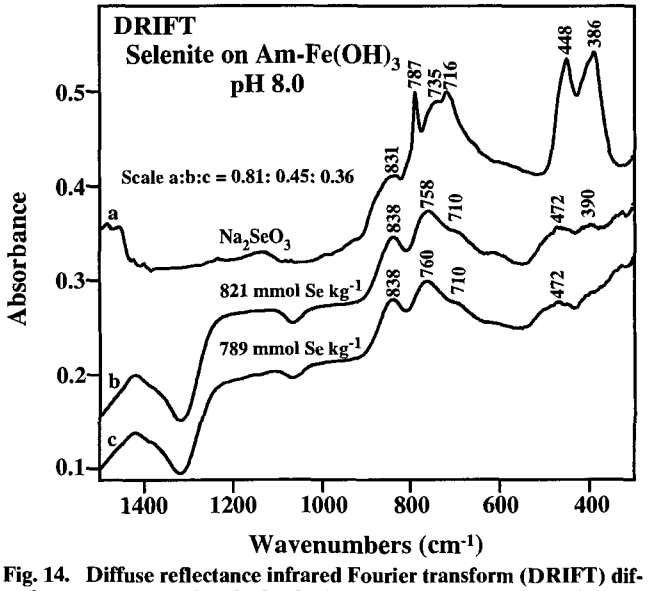

Fig. 14. Diffuse reflectance infrared Fourier transform (DRIFT) difference spectra of sorbed selenite on am-$Fe(OH)_3$ at pH 8.0: (a) analytical grade Na_2SeO_3 and (b) am-$Fe(OH)_3$ reacted with 0.05 *M* Na_2SeO_3 + 1.0 *M* NaCl. The reference spectrum for (b) was the am-$Fe(OH)_3$ equilibrated with 1.0 *M* NaCl.

goethite, however, showed three bands at 911, 885, and 815 cm^{-1}. These bands were assigned to the ν_3 splitting of sorbed selenate. It is concluded that selenate on air-dried goethite also formed bidentate bridging complex. The origin of other bands were not readily explainable.

Characterization of Interfacial Selenite

Chemical properties of selenite in aqueous solution are important in determining selenite complex formation. At low concentrations, the SeO_3^{2-} anion has a pyramidal structure (C_{3v} symmetry) and hydrolyzes to form ($HSeO_3^-$) and selenious acid H_2SeO_3 with $pK_{a1} \approx 2.5$ and $pK_{a2} \approx 8.0$ at room temperature (Fowless and Stranks, 1977). At higher selenite concentrations, extensive dimerization occurs to yield $H(SeO_3)_2^{3-}$, $H_2(SeO_3)_2^{2-}$, $H_3(SeO_3)_2^-$ and $H_4(SeO_3)_2$.

The free SeO_3^{2-} ion has C_{3v} symmetry and absorbs in the region 900 to 350 cm^{-1} (Table 1). There are six fundamental modes of vibration, two pairs of which are degenerate, giving rise to four fundamental frequencies $\nu_1(A_1)$, $\nu_2(A_1)$,$\nu_3(E)$, and $\nu_4(E)$ which are IR active (Fowless and Stranks, 1977). If the selenito ligand were to coordinate through either one or two of its oxygen atoms, then the C_{3v} symmetry would be lowered to C_s symmetry and six fundamental frequencies should be observed. Monodentate and bidentate selenito complexes cannot be distinguished on the basis of the number of fundamental frequencies of the selenito ligand (Fowless and Stranks, 1977). The complexes selenitobis(ethylenediamine)cobalt(III) perchlorate {$[Co(en)_2SeO_3]ClO_4.H_2O$}, and selenitobis(1,3-propanediamine)cobalt-(III) perchlorate{$[Co(tn)_2SeO_3]ClO_4.H_2O$} involve bidentate selenito ligands whose IR spectra include selenito absorptions that are characteristically sharper than those of the monodentate complexes. Moreover, the degenerate $\nu_3(E)$ vibration of free SeO_3^{2-}, which is split on coordination into a doublet for the monodentate selenito complexes, is split into two distinct bands for the bidentate complexes. These qualitative distinctions enable the monodentate and bidentate selenito complexes to be identified (Fowless and Stranks, 1977).

Figure 12 shows the ATR–FTIR spectra of am-$Fe(OH)_3$ reacted at pH 5.0 with 0.5 *M* Na_2SeO_3 + 1.0 *M* NaCl, am-$Fe(OH)_3$ reacted with 1.0 *M* NaCl, and their difference spectrum. The bands at 844 and 750 cm^{-1} are attributed to sorbed selenite. Bands near 1375 and 1485 cm^{-1} are from sorbed monodentate carbonate complex (Su and Suarez, 1997a). Multiple bands at 842, 757, 594, and 478 cm^{-1} were resolved for sorbed selenite at pH 5.0 in the DRIFT difference spectrum (Fig. 13). Similar spectra were observed at pH 8.0 (Fig. 14). Our data suggest a splitting of the ν_3 band (737 cm^{-1}) into the 760, 710 cm^{-1} doublet. These data indicate formation of a selenite surface complex but the question of mono or bidentate complex cannot be resolved with these data alone.

After 4.0 g of am-$Fe(OH)_3$ were reacted with 20 mL of 1.0 *M* Na_2SeO_3 + 1.0 *M* NaCl at pH 5.0 for 24 h, am-$Fe(OH)_3$ was partly transformed to a crystalline iron oxyhydroxide, akaganeite [β-FeOOH], as indicated by the x-ray diffractogram (not shown) and the disappearance of the band at 957 cm^{-1} in the ATR–FTIR spectrum (not shown). In addition, the DRIFT spectrum of the products was in agreement with the IR absorption spectrum of a synthetic akaganeite in a KBr pellet reported by Schwertmann and Cornell (1991). Despite sorbent phase transformation of the am-$Fe(OH)_3$, a large amount of selenite was sorbed.

The ATR–FTIR spectra of goethite reacted with 0.5 and 1.0 *M* Na_2SeO_3 did not show any bands attributable to selenite due to low amounts of sorption by goethite, however, the DRIFT difference spectrum of goethite reacted with 0.1 *M* Na_2SeO_3 at pH 5 showed positive bands for selenite suggesting bridging bidentate complex formation.

Mechanisms of Selenate and Selenite Surface Complexes Formation

We propose mechanisms for selenate and selenite sorption by am-$Fe(OH)_3$ and goethite, based on these observations: (i) the presence of either selenate or selenite lowered the electrophoretic mobility of sorbent particles and decreased the PZC of particles, (ii) the sorption envelope was affected by pH and total Se concentration, (iii) hydroxyl ions were released during both selenate and selenite sorption (Table 2), (iv) the symmetry of sorbed selenate and selenite was lowered as compared to their free species in aqueous solution, and (v) bidentate bridging complex of selenate on wet and air-dried am-$Fe(OH)_3$ surfaces were observed at pH 5.0 and 8.0 as shown by in situ ATR–FTIR spectroscopy and DRIFT spectroscopy (Table 1). Ligand exchange has been proposed as a mechanism for specific (inner-sphere) sorption of anions on oxides (Stumm and Morgan, 1996; Sposito, 1984). It describes the exchange of surface OH groups of a metal cation (≡M) by the aqueous anion (ligand L) as follows:

$$\equiv M{-}OH + L^- = \equiv M{-}L + OH^- \quad [1]$$

The surface OH groups undergo protonation–deprotonation depending on solution pH and ionic strength:

$$\equiv M{-}OH + H^+ + Cl^- = \equiv M{-}OH_2^+ \ldots Cl^- \quad [2]$$

$$\equiv M{-}OH + Na^+ = \equiv M{-}O^- \ldots Na^+ + H^+ \quad [3]$$

The proposed reaction of selenate sorption on am-

Table 2. The molar ratio of hydroxyl release over selenate or selenite sorption for am-$Fe(OH)_3$ after 24 h of reaction.

Treatment	pH	Se sorbed	OH/Se ratio
		mmol kg^{-1}	
1.0 *M* NaCl	5.0	0	–
1.0 *M* NaCl + 0.05 *M* Na_2SeO_4	5.0	313	0.56
1.0 *M* NaCl + 0.1 *M* Na_2SeO_4	5.0	429	0.55
1.0 *M* NaCl	8.0	0	–
1.0 *M* NaCl + 0.05 *M* Na_2SeO_4	8.0	178	0.70
1.0 *M* NaCl + 0.1 *M* Na_2SeO_4	8.0	188	0.94
1.0 *M* NaCl	5.0	0	–
1.0 *M* NaCl + 0.5 *M* Na_2SeO_3	5.0	1382	0.51
1.0 *M* NaCl + 1.0 *M* Na_2SeO_3	5.0	2690	0.53
1.0 *M* NaCl	8.0	0	–
1.0 *M* NaCl + 0.5 *M* Na_2SeO_3	8.0	897	0.87
1.0 *M* NaCl + 1.0 *M* Na_2SeO_3	8.0	1070	0.81

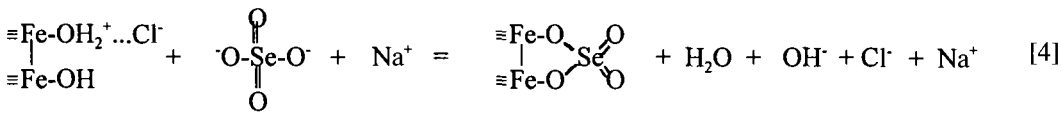

[4]

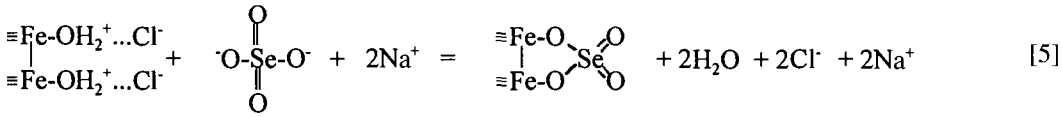

[5]

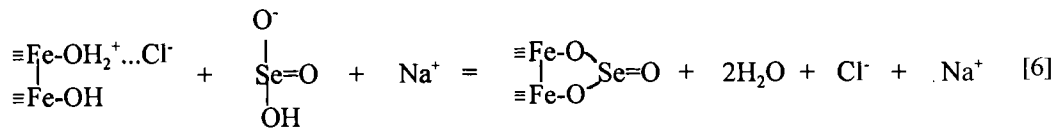

[6]

and

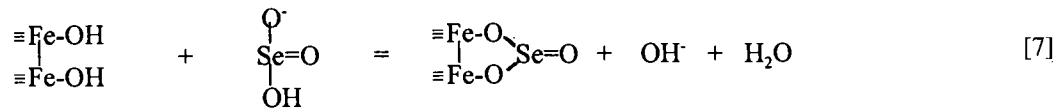

[7]

$Fe(OH)_3$ and goethite is the formation of a bidentate bridging complex with two singly coordinated A-type OH_2^+ groups and OH groups.

The mass action principle (McBride, 1997) helps explain the ionic strength effect. A greater ionic strength (greater NaCl concentration) drives the reactions of Eq. [4] and [5] from right to left, resulting in decreased adsorption of selenate. An increase in ionic strength also lowers the activity of SeO_4^{2-} ion, thus decreasing selenate sorption as shown in Fig. 1 and 2. The greatest ionic strength effect is observed at pH < 8 where the $\equiv Fe\text{-}OH_2^+$ groups predominate (Eq. [5]). Higher pH should decrease selenate sorption and minimize the ionic strength effect as shown in Eq. [4].

No definite mechanism can be derived from the present IR study for selenite on am-$Fe(OH)_3$, although the DRIFT spectra of selenite on am-$Fe(OH)_3$ and goethite suggest bridging bidentate complex. Nevertheless, the release of hydroxyls upon selenite sorption (Table 2), the early EXAFS results of Hayes et al. (1987), and Manceau and Charlet (1994) suggest the reactions in Eq. [6] and [7].

An increase in NaCl concentration should also decrease selenite sorption as Eq. [6] indicates; however, since selenite surface complex is stronger than selenate surface complex as demonstrated by the desorption data, the ionic strength effect is not as significant for selenite as for selenate.

CONCLUSIONS

Similar to other inner-sphere complex forming anions such as phosphate, arsenate, arsenite, borate, and carbonate, the presence of either selenate or selenite lowered the electrophoretic mobility and decreased the PZC of amorphous Fe oxide and goethite. Selenate formed bidentate bridging complexes with am-$Fe(OH)_3$ suspension and air drying seemed to have little effect on the complexation. Sorbed selenite on am-$Fe(OH)_3$ exhibited evidence of complexation as revealed by the DRIFT spectroscopy. Goethite sorbed much less Se than am-$Fe(OH)_3$ on a weight basis. The DRIFT spectra showed the sorbed selenite on amorphous $Fe(OH)_3$ and goethite as likely bridging bidentate complex. A discrete crystalline solid phase, akaganeite, formed when am-$Fe(OH)_3$ reacted with 1.0 *M* Na_2SeO_3 in 1.0 *M* NaCl at pH 5.0 for 24 h. Our results support the conclusions of Manceau and Charlet (1994) that it is not reliable to distinguish between inner-sphere and outer-sphere anion surface complexes by the effects of ionic strength.

REFERENCES

Aochi, Y.O., and W.J. Farmer. 1992. In situ investigation of 1,2-dibromoethane sorption/desorption processes on clay mineral surfaces by diffuse reflectance infrared spectroscopy. Environ. Sci. Technol. 26:329–335.

Balistrieri, L.S., and T.T. Chao. 1987. Selenium adsorption by goethite. Soil Sci. Soc. Am. J. 51:1145–1151.

Barcza, L., and L.G. Sillen 1971. Equilibrium studies of polyanions. 19. Polyselenite equilibria in various ionic media. Acta Chem. Scand. 25:1250–1260.

Barrow, N.J., and A.S. Ellis. 1986. Testing a mechanistic model. V. The points of zero salt effect for phosphate retention, for zinc retention and for acid/alkali titration of a soil. J. Soil Sci. 37:303–310.

Barrow, N.J., and B.R. Whelan. 1989. Testing a mechanistic model. VII. The effects of pH and of electrolyte on the reaction of selenite and selenate with a soil. J. Soil Sci. 40:17–28.

Benjamin, M.M. 1983. Adsorption and surface precipitation of metals on amorphous iron oxyhydroxide. Environ. Sci. Technol. 17: 686–692.

Davis, J.A., and D.B. Kent. 1990. Surface complexation modeling in aqueous geochemistry. p. 177–259. *In* M.F. Hochella and A.F. White (ed.) Mineral-water interface geochemistry. Rev. Mineral. Vol. 23. Min. Soc. Am., Washington, DC.

Dzombak, D.A., and F.M.M. Morel. 1990. Surface complexation modeling: Hydrous ferric oxide. Wiley-Interscience, New York.

Elrashidi, M.A., D.C. Adriano, S.M. Workman, and W.L. Lindsay. 1987. Chemical equilibria of selenium in soils: A theoretical development. Soil Sci. 144:141–152.

Fowless, A.D., and D.R. Stranks. 1977. Selenitometal complexes. 1. Synthesis and characterization of selenito complexes of cobalt(III) and their equilibrium properties in solution. Inorganic Chem. 16: 1271–1276.

Goldberg, S., H.S. Forster, and E.L. Heick. 1993. Boron adsorption mechanisms on oxides, clay minerals, and soils as inferred from ionic strength effects. Soil Sci. Soc. Am. J. 57:704–708.

Goldberg, S., and R.A. Glaubig. 1988. Anion sorption on a calcareous, montmorillonitic soil-selenium. Soil Sci. Soc. Am. J. 52:954–958.

Goldberg, S., and G. Sposito. 1985. On the mechanism of specific phosphate adsorption by hydroxylated mineral surfaces: A review. Commun. Soil Sci. Plant Anal. 16:801–821.

Goldberg, S., C. Su, and H.S. Forster. 1997. Sorption of molybdenum on oxides, clay minerals, and soils: Mechanisms and models. p. 401–426. *In* E.A. Jenne (ed.) Metal adsorption by geomedia: Variables, mechanisms, and model applications. Academic Press, San Diego.

Hansmann, D.G., and M.A. Anderson. 1985. Using electrophoresis in modeling sulfate, selenite, and phosphate adsorption onto goethite. Environ. Sci. Technol. 19:544–551.

Harrison, J.B., and V.E. Berkheiser. 1982. Anion interactions with freshly prepared hydrous iron oxides. Clays Clay Miner. 30:97–102.

Hayes, K.F., and J.O. Leckie. 1987. Modeling ionic strength effects on cation adsorption at hydrous oxide/solution interfaces. J. Colloid Interface Sci. 115:564–572.

Hayes, K.F., C. Papelis, J.O. Leckie. 1988. Modeling ionic strength effects on anion adsorption at hydrous oxide/solution interfaces. J. Colloid Interface Sci. 125:717–726.

Hayes, K.F., A.L. Roe, G.E. Brown, Jr., K.O. Hodgson, J.O. Leckie, and G.A. Parks. 1987. In situ X-ray absorption study of surface complexes: Selenium oxyanions on α-FeOOH. Science (Washington, DC) 238:783–786.

Hunter, R.J. 1981. Zeta potential in colloid science. Academic Press, London.

Hunter, D.B., and P.M. Bertsch. 1994. In situ measurements of tetraphenylboron degradation kinetics on clay mineral surfaces by IR. Environ. Sci. Technol. 24:686–691.

Ihnat, M. 1989. Occurrence and distribution of selenium. CRC Press, Boca Raton, FL.

Letey, J., C. Roberts, M. Penberth, and C. Vasek, 1986. An agricultural dilemma: Drainage water and toxics disposal in the San Joaquin Valley. Div. of Agric. and Natl. Resour. Spec. Publ. 3319. Agric. Exp. Stn., Univ. of California.

Manceau, A., and L. Charlet. 1994. The mechanism of selenate adsorption on goethite and hydrous ferric oxide. J. Colloid Interface Sci. 168:87–93.

McBride, M.B. 1997. A critique of diffuse double layer models applied to colloid and surface chemistry. Clays Clay Miner. 45:598–608.

McNeal, J.M., and L. Balistrieri. 1989. Geochemistry and occurrence of selenium: An overview. p. 1–13. *In* L.W. Jacobs (ed.) Selenium in agriculture and environment. SSSA Spec. Publ. 23. SSSA, Madison, WI.

Nakamoto, K. 1986. Infrared and Raman spectra of inorganic and coordination compounds. 4th ed. John Wiley & Sons, New York.

National Research Council. 1983. Selenium in nutrition. National Academy Press, Washington, DC.

Neal, R.H., and G. Sposito. 1989. Selenate adsorption on alluvial soils. Soil Sci. Soc. Am. J. 53:70–74.

Neal, R.H., G. Sposito, K.M. Holtzclaw, K., and S.J. Traina. 1987a. Selenite adsorption on alluvial soils: I. Soil composition and pH effects. Soil Sci. Soc. Am. J. 51:1161–1165.

Neal, R.H., G. Sposito, K.M. Holtzclaw, K., and S.J. Traina. 1987b. Selenite adsorption on alluvial soils: II. Solution composition effects. Soil Sci. Soc. Am. J. 51:1165–1169.

Nguyen, T.T., L.J. Janik, and M. Raupach. 1991. Diffuse reflectance infrared Fourier transform (DRIFT) spectroscopy in soil studies. Aust. J. Soil Res. 29:49–67.

Parfitt, R.L. 1978. Anion adsorption by soils and soil materials. Adv. Agron. 30:1–50.

Parfitt, R.L., and J.D. Russell. 1977. Adsorption on hydrous oxides. IV. Mechanisms of adsorption of various ions on goethite. J. Soil Sci. 228:297–305.

Parfitt, R.L., and R.S.C. Smart. 1977. Infrared spectra from binuclear bridging complexes of sulphate adsorbed on goethite (α-FeOOH). Chem. Soc. Faraday 73:796–802.

Presser, T.S., and I. Barnes. 1984. Selenium concentration in waters tributary to and in the vicinity of the Kesterson National Wildlife Refuge, Fresno and Merced Counties, California. Water Resour. Invest. Rep. 84-4122. U.S. Geol. Surv., Sacramento, CA.

Presser, T.S., and I. Barnes. 1985. Dissolved constituents including selenium in waters in the vicinity of the Kesterson National Wildlife Refuge and the West Grassland, Fresno and Merced Counties, California. Water Resour. Invest. Rep. 85-4220. U.S. Geol. Surv., Menlo Park, CA.

Rajan, S.S.S., and J.H. Watkinson. 1976. Adsorption of selenite and phosphate on an allophane clay. Soil Sci. Soc. Am. J. 40:51–54.

Ross, S.D. 1972. Inorganic infrared and Raman spectra. McGraw Hill, London.

Ross, S.D., and N.A. Thomas. 1970. Forbidden transition in the infrared spectra of tetrahedral anions-IX: Monodentate selenato complexes. Spectrochim. Acta 26A: 971–975.

Sathianandan, K., L.D. McCory, and J.L. Margrave. 1964. Infrared absorption spectra of inorganic solids-III Selenates and selenites. Spectrochim. Acta 20:957–963.

Schwertmann, U., and R.M. Cornell. 1991. Iron oxides in the laboratory: Preparation and characterization. VCH, New York.

Sposito, G. 1984. The surface chemistry of soils. Oxford Univ. Press, New York.

Stumm, W., and J.J. Morgan. 1996. Aquatic chemistry: Chemical equilibria and rates in natural waters. John Wiley & Sons, New York.

Su, C., and D.L. Suarez. 1995. Coordination of adsorbed boron: A FTIR spectroscopic study. Environ. Sci. Technol. 29:302–311.

Su, C., and D.L. Suarez.1997a. In situ infrared speciation of adsorbed carbonate on aluminum and iron oxides. Clays Clay Miner. 45: 814–825.

Su, C., and D.L. Suarez. 1997b. Boron sorption and release by allophane. Soil. Sci. Soc. Am. J. 61:69–77.

Tan, J., and Y. Huang. 1991. Selenium in geo-ecosystem and its relation to endemic diseases in China. Water, Air, Soil Pollut. 57:59–68.

Tejedor-Tejedor, M.I., and M.A. Anderson. 1986. "In situ" attenuated total reflection Fourier transform infrared studies of the goethite (α-FeOOH)-aqueous solution interface. Langmuir 2:203–210.

Tejedor-Tejedor, M.I., and M.A. Anderson. 1990. Protonation of phosphate on the surface of goethite as studied by CIR-FTIR and electrophoretic mobility. Langmuir 6:602–613.

Van Gee, A., A.P. Robertson, and J.O. Leckie. 1994. Complexation of carbonate species at the goethite surface: Implications for adsorption of metal ions in natural waters. Geochim. Cosmochim. Acta 58:2073–2086.

Wang, P.G., G.L. Ji, and T.R. Yu. 1987. Adsorption of chloride and nitrate by variable charge soils in relation to the electric charge of the soil. Z. Pflanzenernahr. Bodenkd. 150:17–23.

Weighardt, V., and J. Eckert. 1971. Di-μ-sulfato-μ-hydroxo-bis[triamminkobalt(III)]- und Di-μ-selanato-μ-hydroxo-bis[triamminkobalt(III)-komplexe. Z. Anorg. Allg. Chem. 383:240–248.

Zhang, P.C., and D.L. Sparks. 1990. Kinetics of selenate and selenite adsorption/desorption at the goethite/water interface. Environ. Sci. Technol. 24:1848–1856.

Zhang, G.Y., G.M. Brummer, and X.N. Zhang. 1996. Effect of perchlorate, nitrate, chloride and pH on sulfate adsorption by variable-charged soils. Geoderma 73:217–229.